SENSITIVE DEPENDENCE ON THE THRESHOLD FOR TAF SIGNALING IN SOLID TUMORS

D. I. WALLACE AND P. WINSOR

A model of tumor vascularization introduced by Stamper *et al* [8] is further investigated to study the role of a threshold for TAF production by the tumor. This threshold is shown to have three distinct regions which distinguish tumor growth patterns, including a critical region in which the tumor is particularly sensitive to the threshold value. The presence of these regions has implications for tumor classification and potential therapeutic targets.

1. Introduction and Background

A cancer tumor grown *in vitro* reaches a nutrient limitation that gives its growth curve a recognizable logistic or Gompertz curve shape [4]. Tumors growing *in vivo* benefit from vascularization that increases the nutrient supply needed for further growth. The best understood process by which vascularization occurs is *angiogenesis*, the process by which the nearby blood vessels extend into the tumor. The process is believed to be initiated by a substance called *tumor angiogenesis factor* (TAF) which the tumor produces when in a state of hypoxia. TAF acts locally to encourage angiogenesis, but it also circulates in the blood stream and eventually reaches bone marrow. It is suspected that TAF may have a second function of encouraging the formation, delivery and recruitment of *endothelial progenitor cells*, or EPCs, or commonly *stem cells* which can pass to the interior of the tumor and form blood vessels *de novo* which then grow to connect with existing blood vessels. This process, known as *vasculogenesis* is a conjectured second method by which a tumor can increase its access to nutrients. Vasculogenesis in known to happen in developing fetuses, and some researchers claim to have observed and even measured this process in tumors. Thus any model of tumor growth that could shed light on these processes would have to include not only tumor mass, but also vasculature formed in both of these ways, as well as TAF production and the EPC production it is presumed to trigger.

In 2007 Stamper *et al* [8] published such a model. Based on the ba-

sic dynamics just described, it is a system of nonlinear ordinary differential equations in which TAF production is controlled by a threshold above which TAF is produced. This threshold is modeled as a Heaviside function of the tumor mass to vasculature ratio. When that ratio is high, the tumor presumably experiences hypoxia and releases TAF. The form the model takes is well justified by the authors, and whenever possible the constants needed to describe the various rates are taken from values reported in the literature, although these range over a wide variety of tumors. The actual threshold above which TAF is produced in a tumor is not known. The authors are forced to choose it somewhat arbitrarily. They also advise the reader that even the reported constants should not be trusted. However the model exhibits qualitative features that are convincing. In the presence of either or both types of blood vessel creation, the tumor grows substantially faster than in the absence of vascularization. Under some assumptions on local properties of the TAF response Stamper *et al* are able to show multiple equilibrium states for tumors for certain choices of parameter. Oddly, the growth of blood vessels resulting from vasculogenesis is far larger than that resulting from angiogenesis, illustrating the importance of knowing whether this process takes place. Of course, this phenomenon may be a result of the choice of parameters. The authors also investigate the implications of various forms of therapy by altering the growth rates associated to angiogenesis and the death rate of cancer tumor cells, both of which correspond to known forms of therapy.

In this paper we want to take a second look at the signaling threshold, Γ, above which TAF is produced. The dynamics of the model are very sensitive to this parameter, and we show that there are three distinct regions for this parameter characterized by very different behaviors of the model. Section 2 describes the model and its modifications, section 3 describes the computer simulation used to study the model and section 4 describes the basic results. Section 5 discusses the results in more detail as well as implications for further research.

2. The original model of Stamper *et al*, and modifications

In the following model, m represents tumor mass, x, y and z represent EPC's in the bone marrow, blood and tumor mass respectively, w and u represent tumor vasculature formed by angiogenesis and vasculogenesis respectively, and C_1, C_2 and C_3 are quantities of TAF in the tumor, blood, and bone marrow respectively. Equations 1-9 describe the model studied in

this paper, based on Stamper *et al* [8] with some modifications as described below.

Tumor mass distinct from vasculature, (m), grows in this model via two processes. The both positive growth terms lead to an equilibrium in the presence of vasculature. The second was added to allow for limited growth in the absence of vasculature, as observed in *in vitro* studies.

$$\frac{dm}{dt} = \frac{\beta(v_0+u+w)m}{(v_0+u+w)+\lambda m} - d_0 m + \alpha m(1 - \frac{m}{(b_0+v_0+u+w)}) \quad (1)$$

EPCs in the bone marrow, x, are created at a constant rate independent of TAF signaling (p_1) as well as in response to that signaling (p_2C_3). They are removed from the bone by delivery into the blood at a constant relative rate independent of TAF production (k_1x) and additionally a rate dependent on the TAF differential from bone to blood ($k_2(C_2 - C_3)x$). Additionally these cells may die (apoptosis, d_1x).

$$\frac{dx}{dt} = p_1 + p_2C_3 - k_1x - k_2(C_2 - C_3)x - d_1x \quad (2)$$

EPCs in the blood, y, enter from the bone marrow ($k_1x+k_2(C_2-C_3)x$). They may exit into the tumor in proportion to their number, TAF signaling, and available vasculature ($k_3C_1(v_0+u+w)y$), or they may die (d_2y).

$$\frac{dy}{dt} = k_1x + k_2(C_2 - C_3)x - k_3C_1(v_0+u+w)y - d_2y \quad (3)$$

EPCs in the tumor, z, arrive from the blood ($k_3C_1(v_0+u+w)y$), may proliferate within the tumor in response to TAF presence (p_3C_1z), may align themselves into existing tissue (k_4z) or may die (d_3z).

$$\frac{dz}{dt} = k_3C_1(v_0+u+w)y + p_3C_1z - k_4z - d_3z \quad (4)$$

Angiogenesis generated vasculature, w, arises via proliferation in response to TAF signaling ($p_4C_1(v_0+w)$). This vasculature is lost by apoptosis (d_4w) and by occlusion ($\frac{\delta_1 mw}{m+\delta_2(u+w+v_0)}$), the process by which blood vessels close due to pressure from the surrounding tissue. Occlusion is modeled as a Hill function in m/v, giving a small effect when there is high density of vasculature in the tumor and rising to a maximum rate as m/v grows.

$$\frac{dw}{dt} = p_4 C_1(v_0 + w) - \frac{\delta_1 m w}{m + \delta_2(u + w + v_0)} - d_4 w \tag{5}$$

Vasculogenesis generated vasculature, u, is presumed to begin when an EPC cell adheres to the tumor and produces vasculature ($\mu k_4 z$), or when it proliferates in response to TAF ($p_5 C_1 u$). This vasculature is also lost by apoptosis ($d_5 u$) and by occlusion ($\frac{\delta_3 m w}{m+\delta_2(u+w+v_0)}$).

$$\frac{du}{dt} = \mu k_4 z + p_5 C_1 u - \frac{\delta_3 m u}{m + \delta_4(u + w + v_0)} - d_5 u \tag{6}$$

The tumor begins TAF, (C_1), production in response to hypoxia governed by m/v. This is modeled by a Heaviside function ($cmH(m - \Gamma v)$). TAF is released into the blood in response to the TAF differential of tumor and blood ($q_1 v(\frac{C_1}{\gamma_1} - C_2)$). The process is scaled by the total volume of the tumor ($((v_0 + w + u + m)^{-1})$).

$$\frac{dC_1}{dt} = ((cmH(m - \Gamma v) - q_1 v(\frac{C_1}{\gamma_1} - C_2))((v_0 + w + u + m)^{-1}) \tag{7}$$

TAF in the bloodstream, (C_2), is assumed to enter the blood in proportion to available tumor vasculature, ($(v_0 + w + u + m)$) and the TAF differential from tumor to blood ($(\frac{C_1}{\gamma_1} - C_2)$). It passes from blood to bone marrow in response to TAF differential ($Q_3(C_2 - \frac{C_3}{\gamma_3})$) and is lost via pharmacokinetic decay (rC_2). The process is scaled by the total volume of blood (V_2^{-1}) which is assumed to remain constant.

$$\frac{dC_2}{dt} = ((q_1(v_0 + w + u + m)(\frac{C_1}{\gamma_1} - C_2) - Q_3(C_2 - \frac{C_3}{\gamma_3}) - rC_2))(V_2^{-1}) \tag{8}$$

TAF in the bone marrow, (C_3), is assumed to enter the bone in proportion to TAF differential ($Q_3(C_2 - \frac{C_3}{\gamma_3})$) and is scaled by the total volume of bone marrow (V_3^{-1}) which is assumed to remain constant.

$$\frac{dC_3}{dt} = (Q_3(C_2 - \frac{C_3}{\gamma_3}))(V_3^{-1}) \tag{9}$$

We now delineate alterations made above to the model of Stamper *et al* [8].

2.1. *Growth without vasculature*

In the absence of vasculature, tumor growth is severely restricted by access to nutrients and has been observed to follow a Gompertz or logistic curve[4]. We altered the growth term so that it reduces to the logistic equation in the absence of vasculature. This is only somewhat more accurate that the term used in Stamper *et al*, which also rises to an equilibrium in the absence of vasculature.

2.2. *Heaviside trigger* Γ

Stamper *et al* replace the trigger for signaling with an approximation. We were using a recent version of the Matlab ode45 solver that could incorporate the Heaviside function directly without ruining the conditioning of the numerical solution, so we did not need to use the an approximation.

2.3. *The assumption of TAF equilibrium*

Stamper *et al* reduce the dimensionality of their model by assuming that TAF quantities approach equilibrium quickly. They replace the equations describing these three quantities with their values at (pseudo) equilibrium. This simplification allows them to compute and analyze system equilibria. We were particularly interested in the role of the signaling parameter, which is connected directly to TAF production, so we kept these equations close to their original form. The units were interpreted as TAF concentration per unit volume (of tumor, blood, and so forth). This allowed a slight simplification in the case of C_1 from the original model. We note that the equilibrium assumption of the original equations, duplicated here, gives the same equilibrium result due to the assumptions made by those authors. However, no assumptions of TAF equilibrium were made in the simulations in this study.

3. Methods

The full model was programmed using Matlab's ode45 solver. Various numerical runs gave parameter values that reasonably approximated the output of Stamper *et al*. The program was then run across a range of values for Γ and output was saved to a master file and mined for interesting relationships. All runs had default starting values as given in Table 2. The program was run until $t = 40$ in all cases.

Vasculature Regs defvals2.jpg

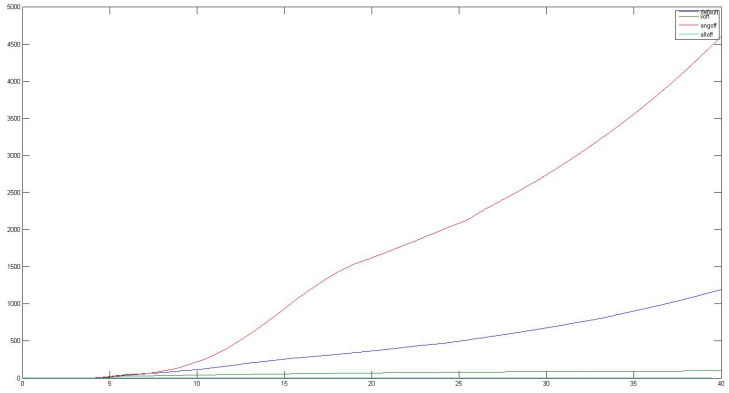

Figure 1. The model with 1. vasculogenesis only (top curve), 2. both vasculogenesis and angiogenesis (second from top), 3. angiogenesis only (third from top) and 4. no vasculature growth (bottom curve barely visible). All other parameters are at default values.

Compare.jpg

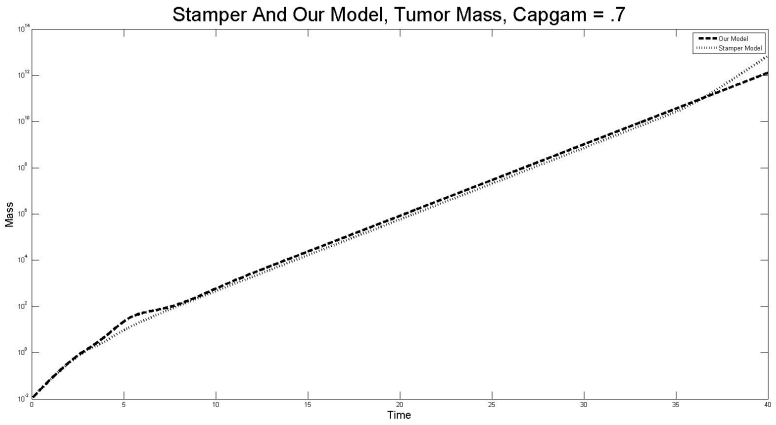

Figure 2. The darker graph is the model described in this paper. The lighter is the original model run in Stamper *et al.* Both are at $\Gamma = .7$ and other parameters at default values.

Table 1. Default parameter values

Parameter	symbol	default value
max tumor growth rate	β_0	.7
production rate of TAF per unit tumor volume	c	1
relative rate of death	d	.3
tumor relative rate of death	d_0	.3
bone EPC relative rate of death	d_1	.2
blood EPC relative rate of death	d_2	.2
tumor EPC relative rate of death	d_3	1
angiogenic vasculature relative rate of death	d_4	.2
vasculogenic vasculature relative rate of death	d_5	.3
maximum rate of angiogenic vasculature occlusion	δ_1	.2
half saturation of angiogenic vasculature occlusion	δ_2	1
maximum rate of vasculogenic vasculature occlusion	δ_3	.2
half saturation of vasculogenic vasculature occlusion	δ_4	.1
scaling factor for TAF delivery	γ_1	1
scaling factor for TAF delivery	γ_2	1
scaling factor for TAF delivery	γ_3	1
TAF signaling threshold	Γ	1
bone to blood relative rate of EPC delivery	k_1	1
bone to blood relative rate of EPC delivery per unit TAF	k_2	1
relative rate of adherence of EPCs per unit TAF and unit vasculature	k_3	1
relative rate of alignment of EPCs into tumor vasculature	k_4	.2
half saturation of tumor growth rate	λ	1
vasculature volume per EPC	μ	1
constant rate of EPC production in bone	p_1	1
relative rate of extra EPC in bone production per unit TAF	p_2	1
relative rate of extra EPC production at tumor site per unit TAF	p_3	1
relative rate of angiogenic production per unit TAF	p_4	1
relative rate of vasculogenic production per unit TAF	p_5	1
blood flow to tumor per unit vasculature	q_1	1
blood flow to bone marrow	Q_3	1
decay rate of TAF in blood	r	.1
initial vasculature	v_0	.01
volume of blood (constant)	V_2	.005
volume of bone marrow (constant)	V_3	$5e^{-.05}$

Table 2. Default initial conditions

Quantity	symbol	initial value
TAF concentration in tumor	C_1	0
TAF concentration in blood	C_2	0
TAF concentration in bone	C_3	0
tumor size	m	.01
vasculogenesis driven vasculature	u	0
angiogenesis driven vasculature	w	0
EPCs in bone marrow	x	1.4286
EPCs in bloodstream	y	3.5714
EPCs in tumor	z	0

4. Results

4.1. *Behavior of the model in under various assumptions on vasculature growth*

Typical runs of the system are shown in Figure 1, which displays tumor growth under the assumption of both angiogenesis and vasculogenesis, as well as showing the result of considering each separately. This run was typical of output that suggested vasculogenesis was a bigger contributor to vasculature. Because the mechanism of occlusion is included in the model, new vasculature can be crowded out by existing organs (including the vasculature itself). Perhaps this is why a model only including vasculogenesis produced a larger tumor mass at 40 days than one incorporating both processes.

The results we see here are reasonably close to the original Stamper *et al* model.

4.2. *The assumption of TAF equilibrium, the use of the Heaviside function and the term involving tumor growth without vasculature*

Working from our model backwards using the default parameters, we can reproduce the assumptions of Stamper *et al*. We replace our growth term with their original one, replace the differential equations for TAF production with the computed pseudo-equilibrium values, and replace the Heaviside function with an approximation. We see the result of this experiment in Figure 2.

We would expect the term describing growth in the absence of vasculature only affects the very early part of the graph and any such effect is

nearly invisible in this figure. For most of the run the two models perform similarly.

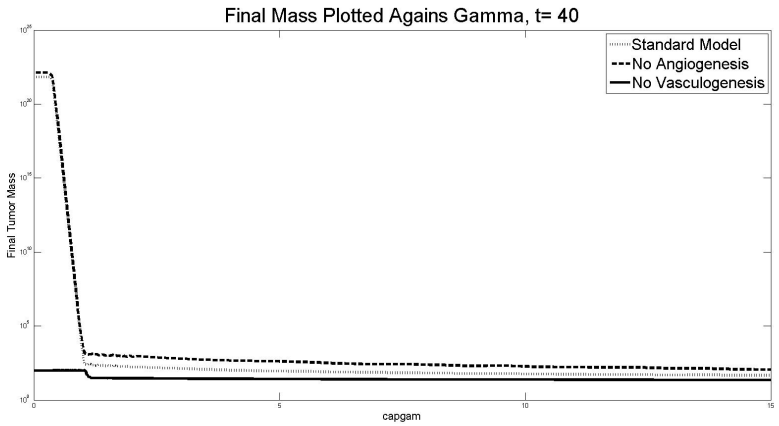

Figure 3. The signaling threshold Γ was varied from 0 to 15 and all other parameters kept constant. Above (approximately) $\Gamma = 3$, the mass at $t = 40$ varies little. Also at low values of Γ (below approximately .5) the mass stabilizes at a higher value. All other parameters are at the default values.

4.3. *Mass to Vasculature and m versus* Γ

As the signaling threshold, Γ, was varied across a range of values, some interesting properties emerged. Figure 3 shows tumor mass at $t = 40$ as Γ ranges from near 0 to 15. We see three distinctly different regions of behavior. Low values of Γ correspond to signaling at relatively low levels of hypoxia, as measured by vasculature to mass ratio, and results in a higher growth rate of the tumor. Very high values of Γ make it harder for the tumor to signal at all. An intermediate region, running roughly from $\Gamma = .5$ to $\Gamma = 3$ shows a very steep slope. In this region the tumor is particularly sensitive to changes in Γ. Hereafter we refer to this region as the *critical interval* for Γ.

Figure 4 shows the same range of Γ but plots the ratio of tumor mass to total vasculature, the quantity that signals hypoxia and triggers TAF production in this model. Again we see three distinct regions of behavior. Predictably, the increasing threshold for signaling results in increasing mass

to vasculature. In the critical interval the rate of increase is extremely high. Note that the graphs pictured include runs with angiogenesis only, those with vasculogenesis only, and the standard model containing both types of vessel formation. All of these cases show the same critical interval and similar qualitative properties.

Mass Over Vasculature against Gamma2.jpg

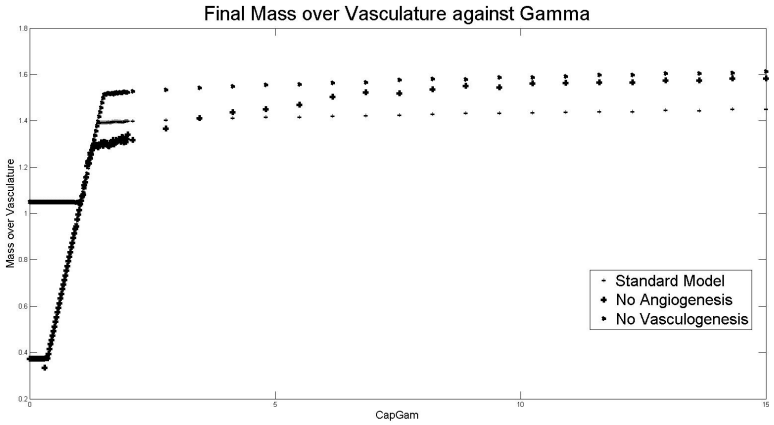

Figure 4. The signaling threshold Γ was varied from 0 to 15 and all other parameters kept constant. Above (approximately) $\Gamma = 3$, the mass to vasculature ratio stabilizes. Also at low values of Γ (below approximately .5) the ratio stabilizes at a lower value. All other parameters are at the default values.

Not only do final mass and mass to vasculature ratio change rapidly in the critical region, but so does the relationship between the two quantities, as shown in Figure 5. These are the same data points, but here we see a region where mass to vasculature drops steeply without much increase in final mass, followed by a nearly linear relationship of steady descent as mass to vasculature drops but final mass rises steadily.

4.4. *Behavior of* Γ *in the critical interval*

Figures 3-5 lead one to suspect that at low values of Γ the threshold is always surpassed, TAF production is constant, and final mass only differs because of the slight lead time in vessel formation offered to the tumor with lower Γ. Similarly, one suspects that at high values of Γ, the signal is always off, and vascular growth as well as tumor growth depend only on

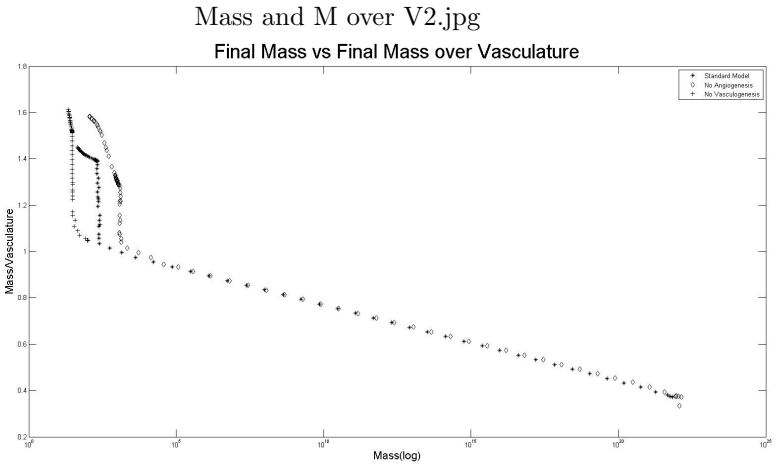

Figure 5. The signaling threshold Γ was varied from 0 to 15 and all other parameters kept constant. All other parameters are at the default values. Low values of Γ correspond to the cluster of points with very high mass. High values of Γ correspond to the top of the vertical traces at the left of the diagram with relatively constant mass. Γ in the critical region corresponds to the curves of steep descent of the mass to vasculature ratio.

the remaining EPC production and resulting vasculogenesis. To test this, the model was run for four values of Γ, two of which are in the critical interval. In Figure 6 we see the result. A solid line indicates that the mass to vasculature ratio is above 90% of Γ. This approximates intervals in which signaling would occur. As expected, signaling is always on for the lowest value of Γ, off for the highest, and switching on and off constantly in the critical interval.

The mechanism of TAF production is modeled by a Heaviside function because it is thought to be a biological switch that turns a process on and off according to the needs of the organism. In fact it is only in the critical interval that it actually behaves as a switch. Outside this interval it remains in one state.

4.5. *Sensitivity of the model to parameter values*

Figures 3-5 also suggest that the system is particularly sensitive to Γ. We conducted a sensitivity analysis around the default parameters given in Table 1. Each parameter was varied by ten percent up or down and the resulting change in final tumor mass was compared across all parameters.

Compares.jpg

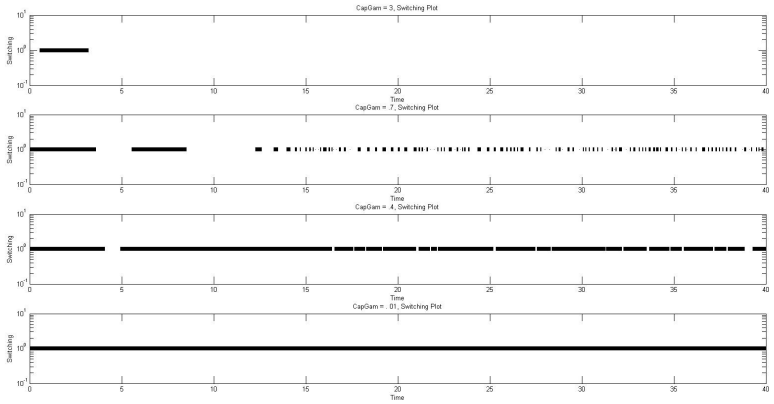

Figure 6. The signaling is shown for Γ at 3, .7, .4 and .01. At $\Gamma = 3$ the signal is nearly always off, and at $\Gamma = 1$ it is always on. At intermediate values it switches on and off repeatedly.

The system was most sensitive to Γ by several orders of magnitude. A ten percent increase in Γ resulted in a 400% increase in final tumor volume. Figure 7 summarizes the result, showing only the most influential parameters in descending order.

5. Discussion

The usefulness of a model such as this one is its potential for providing testable hypotheses and suggesting avenues of further research. In this section we point out some of the implications of the results outlined above.

5.1. *Critical interval for* Γ

The parameter Γ controlling the threshold for TAF signaling divides tumor growth into three distinct classes: those for which TAF signaling is always on, those for which it is always off, and a critical interval in which signaling switches on and off. These three intervals have distinctive growth signatures in terms of final mass, final mass to vasculature ratio, and the ratio of those two quantities as in Figures 3-5. The model suggests the possibility of looking for these signatures in actual tumors. Several methods are now available for measuring the amount of vasculature in a tumor [3 7 5], so that

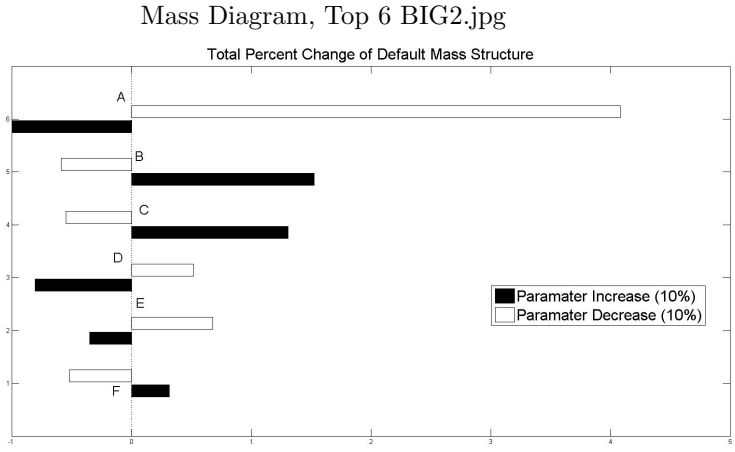

Figure 7. All parameters were varied by ten percent (one at a time) from the default values. The diagram shows the variation in tumor mass at 40 days from the default run for the six largest differences. The system was most sensitive to $A = \Gamma$, with the tumor mass increasing by 400 % for a ten percent decrease in Γ. Other parameters are: $B = \beta_1$ (tumor growth rate), $C = d_0$ (tumor death rate), $E = \lambda$ (half saturation of tumor growth rate), $F = p_3$ (rate of EPC production at tumor site).

tumors of similar age could be compared on this basis. A statistical analysis should be able to identify at least the two extreme cases outside the critical interval clearly.

Similarly, Figure 6 suggests that the action of Γ on the system could be identified by TAF measurements. At least one substance, VEGF [1], is known to function as a TAF, and measurements indicate higher levels of it in some patients with some tumors. If the concentration of a TAF could be measured over time, it would be possible to identify whether it remains relatively low, relatively high, or whether it oscillates in response to a switching signal as suggested by this model. Such phenomena could be compared with tumor growth rates to verify the model proposed by Stamper *et al* and investigated here.

5.2. *The presence of TAF pseudo-equilibria, and other equilibrium considerations*

For ease of calculation, Stamper *et al* make the assumption that TAF concentrations rapidly reach a pseudo-equilibrium. Based on this assumption

they are able to compute bifurcation diagrams for the angiogenesis and vasculogenesis submodels. A crucial step in this calculation shows that, under their assumptions, TAF signaling is either always on or always off. In the case it is off, the model goes has a stable equilibrium. When TAF signaling is always on, there are two equilibria, one stable and one unstable. The unstable equilibrium marks a boundary between those initial conditions that drop to a vascularized equilibrium state and those that grow unbounded. The bifurcation parameter is the ratio of maximum tumor growth rate to tumor apoptosis rate, and the point of bifurcation is determined by Γ. They could equally well have fixed the growth/death ratio and adjusted Γ instead.

Our analysis shows that, without the assumption of TAF pseudo-equilibrium, the dynamics are quite different in the critical interval for Γ, as the signal is never completely on or off, but switches. This remains true whether we look at the standard (combined) model, or whether we look at the angiogenesis and vasculogenesis submodels. The analysis also shows greater sensitivity when Γ is perturbed than any other parameter. So rather than an abrupt bifurcation and instant rise to a higher equilibrium in the presence of TAF generation, we see a region of rapid increase of final mass as the system signals more often. We did not observe any equilibrium values reached when vasculogenesis was present, as in the typical run pictured in Figure 1.

Finally we observe that the biological switch represented by the Heaviside function only exhibits switching behavior in the critical interval. This behavior is somewhat more believable than TAF production that is always on or always off, as we know that normal tissue development would require a more sensitive response.

5.3. *On the Contribution of Vasculogenesis versus Angiogenesis*

Figure 1 shows a big difference of final mass between the angiogenesis submodel and either model containing vasculogenesis. It almost appears as if the angiogenesis submodel is indeed reaching an equilibrium. This would provide a big distinction between a system with vasculogenesis and one without it. Evidence for or against vasculogenesis might therefore be inferred from known tumor behaviors.

In particular, it would be useful to know whether the angiogenesis submodel really does go to equilibrium, even in the critical interval of Γ. Figure

6 shows some of the switching patterns in this interval. It may be possible to approximate this pattern by a linear random switching system such as those described in Dayawansa *et al* [2] and Liberzon *et al* [6]. . These are basically two linear systems describing the same phenomenon with a probabilistic switch between them. Some of these systems can be shown to approach an equilibrium dependent on the probabilities associated to each of the systems involved. Perhaps the angiogenesis submodel could be analyzed in this fashion and shown to possess a stable equilibrium.

5.4. *Further Implications*

We see in this model tremendous sensitivity to a single parameter, the signaling threshold for TAF production. It is natural to wonder whether there is much natural variation in this parameter between individuals, whether tumors have set this threshold at a different level than healthy tissue, and to what extent it is malleable and hence a therapeutic target. The model also suggests a method for categorizing tumors according to this threshold, which may be inferred by final mass and mass to vasculature ratio.

Acknowledgments

The authors wish to acknowledge the Dartmouth College Ordinary Differential Equations class of Winter 2010 for its assistance in exploring various versions of the model presented here.

References

1. T. Asahara, T. Takahashi, H. Masuda, C. Kalka, D. Chen, H. Iwaguro, Y. Inai, M. Silver & J. M. Isner, *EMBO J.* **18 14**, 3964-3972, (1999)
2. W.P. Dayawansa & C. F. Martin, *IEEE Transactions on Automatic Control* **44 4**, 751-760, (1999)
3. M. Dellian, B.P. Witwer, H.A. Salehi, F. Yuan % R. K. Jain, *Am. J. Pathology* **149 1** 59-71 (1996)
4. E. Demidenko, *J. Royal Statistical Soc. Series C* **55 3**, 365-377, (2006)
5. E. F. Donnelly, L. Geng, W. E. Wojcicki, A. C. Fleischer, D. E. Hallahan, *Radiology* **219**, 166-170, (2001)
6. D. Liberzon, J. P. Hespanha & S. Morse *Systems & Control Letters* **37 3**, 117-122, (1999)
7. M. A. Lodge, H. A. Jacene, R. Pili, R. L. Wahl, *J. Nucl Med.* **49 10**, 1620-1627, (2008)
8. I.J. Stamper, H.M. Byrne, M.R. Owen & P.K. Maini *Bull. of Mathematical Biology* **69** 2737-2772, (2007)